Chinese Chemical Letters 33 (2022) 1445–1449

Contents lists available at ScienceDirect

Chinese Chemical Letters

journal homepage: www.elsevier.com/locate/cclet

Light-mediated CO_2-responsiveness of metallopolymer microgels

Xiaofei Wang[a,1], Xuezhen Lin[a,1], Huijuan Qiu[a], Jianda Xie[b], Zhengyu Lu[a], Yusong Wang[c], Weitai Wu[a,d,*]

[a] State Key Laboratory for Physical Chemistry of Solid Surfaces, Collaborative Innovation Center of Chemistry for Energy Materials, The Key Laboratory for Chemical Biology of Fujian Province, and Department of Chemistry, College of Chemistry and Chemical Engineering, Xiamen University, Xiamen 361005, China
[b] School of Materials Science and Engineering, Xiamen University of Technology, Xiamen 361024, China
[c] Hefei National Laboratory for Physical Sciences at the Microscale, University of Science and Technology of China, Hefei 230026, China
[d] School of Chemistry and Chemical Engineering, Ningxia University, Yinchuan 750021, China

ARTICLE INFO

Article history:
Received 17 June 2021
Revised 4 August 2021
Accepted 11 August 2021
Available online 17 August 2021

Keywords:
Stimuli-responsive
Metallopolymers
Light
Dilute CO_2
Reversible uptake-release

ABSTRACT

Here, we report a finding on light-mediated CO_2-responsiveness. It is found on the microgels that are made of side-chain type metallopolymers containing metalla-aromatics. Turbidity and laser light scattering studies on dilute aqueous dispersion of these microgels in dark indicate high CO_2-responsivity, but poor reversibility upon N_2 purge, which can be improved by exposing to light. This light-mediated CO_2-responsiveness can be elucidated by the loss of aromaticity from initial photoexcitation and concurrent formation of a less reactive, antiaromatic excited state of relatively low CO_2 binding affinity, and by subsequent relief of antiaromaticity that can enhance the CO_2 removal. The finding is also checked by CO_2 uptake-release experiments on the microgels, which enables both CO_2 capture of high capacity and CO_2 removal of good reversibility under a mild condition, allowing effective and reversible response to dilute CO_2.

Stimuli-responsive polymeric materials that can reversibly respond to CO_2 provides great opportunities [1–6]. Besides the prospect of CO_2 capture and removal in easing the world's energy and environmental problems, with CO_2 as a stimulus to induce polymer phase transitions, it is able to regulate properties of CO_2-responsive polymeric materials for cell mimics, drug delivery, and many other applications [6–12].

Because of the prospective applications, efforts have been made to explore fundamental principles of polymer design to enable CO_2-responsiveness, including the choice of CO_2-responsive moieties and how effective CO_2-responsiveness can be expected to be under the conditions of interest [11,12]. Up to now, CO_2-responsive polymeric materials are principally synthesized by the functionalization of polymer chains with basic groups, which can react with acidic CO_2 in water based on acid–base pair theory [7–11]. Owing to reversible nature of the acid–base equilibrium, CO_2 can be removed by bubbling with inert gases (*e.g.*, N_2 gas) under a mild condition. This offers an advantage of free of contamination by accumulated chemicals; yet, it also makes the materials barely respond to dilute CO_2, due to low capacity of the CO_2-responsive polymeric materials for CO_2 capture from dilute CO_2 sources, which undisputedly is a critical drawback [1–12]. As a theoretical possibility, enhancing CO_2 binding affinity might allow CO_2 capture of high capacity [13–16], which paves the way to address this problem [11] and thus have recently received attention in CO_2-responsiveness design [17,18]. For instance, efforts are made by exploiting frustrated Lewis pair (FLP) [19], and use CO_2 to bridge FLP-containing polymers *via* dynamic covalent bonding [17,18]. However, high CO_2 binding affinity in turn leads to difficulty in CO_2 removal without heating ($\geq$ 60 °C typically). The challenge of seeking stimuli-responsive polymeric materials of a distinct mechanism to allow both CO_2 capture of high capacity and CO_2 removal of good reversibility under a mild condition remains to be solved.

In this work, we would like to report a concept of how to tune CO_2 binding affinity to mediate CO_2-responsiveness by using side-chain type metallopolymers containing metalla-aromatics as CO_2-responsive moieties on microgels. Unlike bases or FLP groups reported in previous articles that give rise to intra-/intermolecular acid-base activation of CO_2 *via* ionic or dynamic covalent bonding [1–14], metallopolymers (or organometallic polymers) with metal functionalities display typically high CO_2 binding affinity *via* strong interactions (*e.g.*, metal complexes) [20–22], which however are

* Corresponding author.
E-mail address: wuwtxmu@xmu.edu.cn (W. Wu).
[1] These authors contributed equally to this work

https://doi.org/10.1016/j.cclet.2021.08.051
1001-8417/

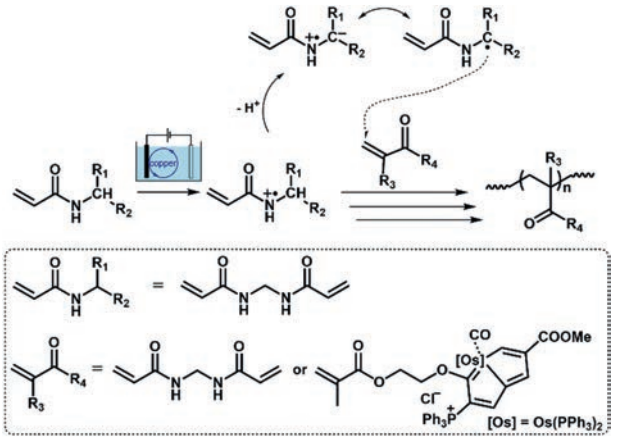

Scheme 1. Synthesis of metallopolymer microgels.

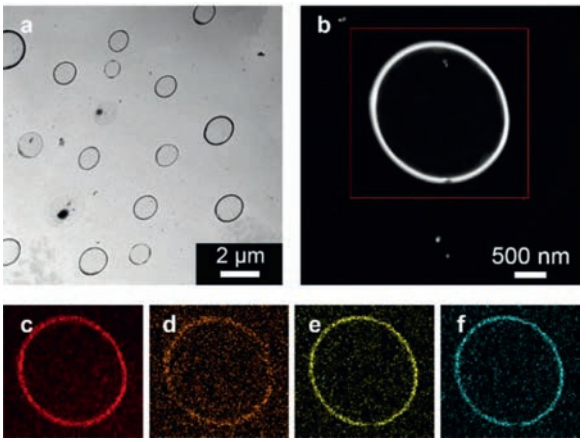

Fig. 1. (a, b) TEM images of the microgels. (c–f) Typical EDX elemental mapping of (c) carbon, (d) oxygen, (e) phosphorus, and (f) osmium on the single gel particle shown in (b).

rarely used for harnessing CO_2-responsiveness. Here our intention to use those metallopolymers containing metalla-aromatics is because most metalla-aromatics are thermodynamic stable and possess properties of both organometallics and aromatics [23,24]. An alteration in (anti)aromaticity is known to efficiently tune reactivity [25]. For instance, (anti)aromaticity can promote reactivity of FLP groups with small molecules like CO_2 [26,27]. Interestingly, light exposure could lead to a change in (anti)aromaticity, offering a facile way to vary reactivity [28–30]. This tunning in reactivity may depend on a combination of properties: the number of electrons, the orbital topology, and the electronic state, in the sense that a change in each of these factors lead to a reversal in the allowedness and forbiddenness; in particular, the results pointed to a reversal of (anti)aromaticity following photoexcitation [28–30]. Inspired by these, one wonders if it is possible to obtain polymeric materials, microgels [3,31–33] here of metallopolymers containing metalla-aromatics, of effective and reversible CO_2-responsiveness by utilizing light as a mediator (Scheme 1).

The microgels were synthesized through electrochemical polymerization [34] of a Craig-type coplanar Möbius metalla-aromatic compound (OsHEMA; 2.0×10^{-4} mol/L) [35] with a crosslinker *N,N*'-methylenebisacrylamide (MBAAm; 2.0×10^{-6} mol/L), and with copper nanoparticles (36 ± 5 nm; see Fig. S1 in Supporting information for TEM, XRD and UV-vis absorption results) as mediators for electron transfer, so as to avoid direct electrolysis of OsHEMA on the electrode that might lead to disproportional reactions [36]. On an anodic scan, an oxidation starts to develop on copper nanoparticles at a low potential of *ca.* +0.2 V *versus* Ag/AgCl (Fig. S2 in Supporting information), leading to formation of strong oxidizing copper species [36,37], which can attack MBAAm to form N-localized radicals [34,36]. These N-localized radicals could trigger a cascade of reactions that typically involve the loss of a proton and formation of C-localized radicals, which then initiate polymerization on attacking vinyl groups of the monomer/crosslinker, making them enter into free radical polymerization [36] and particle growth processes in the electrochemical systems [34,38]. In this circumstance, the synthesis should proceed upon applying a suitable potential of +0.3 V that is above the oxidation wave of copper nanoparticles, but below those of OsHEMA (starting at *ca.* +0.6 V *versus* Ag/AgCl) and MBAAm (starting at +1.6 V *versus* Ag/AgCl) (Fig. S3 in Supporting information), resulting in toroidal-like microgels (collected after reacting for 4 h at 25.0 °C, and purified before characterization; Fig. 1a). The mean diameter of freeze-dried toroids is 1.46 ± 0.21 μm, and the width is 69 ± 23 nm; the outline is barely sharp due to the existence of corona [34,39] on surface that may be indistinctly seen in Fig. 1b. Energy dispersive X-ray (EDX) elemental mapping results indicated the existence of carbon, oxygen, phosphorus and osmium in an individual toroid; no copper salts or other inorganics were detected (Figs. 1c-f). The edge of EDX elemental maps matches well that in annular dark-field TEM image (Fig. 1b), indicating that those elements and corresponding moieties are distributed throughout microgels. ^{31}P NMR spectrum of the microgels (Fig. S4 in Supporting information) showed two signals of the metalla-aromatic moiety at *ca.* 13.0 (for $CPPh_3$) and 3.6 ppm (for $OsPPh_3$), and in ^{1}H NMR spectrum (Fig. S5 in Supporting information) at *ca.* 12.2 (for OsCH) and 7.1-8.2 ppm (for other aromatic protons) [35], indicating the integration of the metalla-aromatic moiety to the microgels. The weight percentage of the metalla-aromatic moiety was estimated to be *ca.* 95.4 wt%, *via* analyzing the percentage of osmium metal by inductively coupled plasma mass spectrometry [35], which was close to the feeding for microgel synthesis (*ca.* 99.9 wt%). The microgels were hydrophilic (Fig. S6 in Supporting information) and kept stable in water (Fig. S7 in Supporting information). To verify the shape and composition of microgels (Table S1 in Supporting information), over five samples were repeated, and ten samples were prepared at 20–30 °C, which displays negligible influence on synthesis. The microgels were reproducible from batch to batch, with an average yield of ≥ 80%.

Phase diagrams for aqueous microgel dispersion (0.015 wt%) were studied by UV-vis spectroscopy at a wavelength $\lambda = 700$ nm (of incident light intensity I_0), where absorption is negligible (Fig. S8 in Supporting information). The decrease in transmitted light intensity (I_T) can be associated with scattering, to give the normalized attenuation coefficient δ_λ as [34]:

$$\delta_\lambda = D_\lambda/(c \cdot d) \quad (1)$$

where the light attenuation $D_\lambda = \lg(I_0/I_T)$, c for the microgel concentration (wt%), and d for the cuvette thickness (1 cm). The tests were made at a slow temperature ramp (3 °C/h; using a temperature controller, ±0.1 °C) followed by a long waiting (30 min, after temperature reaching equilibrium) and a rapid measurement time (< 1 s), to ensure in the equilibrium state of microgels at each measurement. The dispersion was bubbled with N_2 or CO_2 gas (20.0 mL/min under 1 atm in dark) and equilibrated in a cuvette for tests. Upon purge with CO_2 at a set temperature in the range of 20–80 °C, the δ_{700} changed immediately and reached equilibrium within 30 min of CO_2 purge (Fig. S9 in Supporting information), and the δ_{700} (equilibrated; the same below) increased with the amount of CO_2 going through the dispersion *via* adjusting purge time (Fig. 2a). The increase in the δ_{700} is possibly associated with the binding of CO_2 to the metalla-aromatic moiety

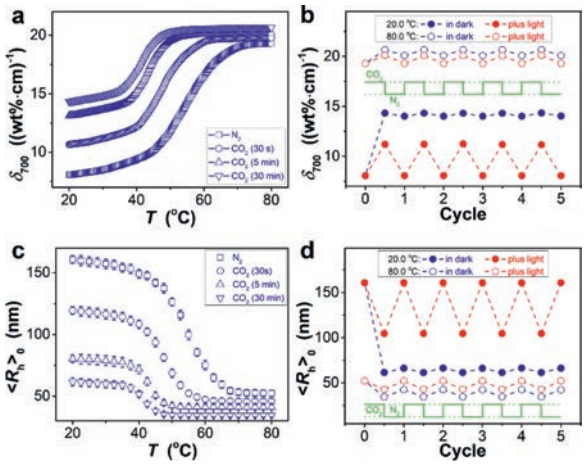

Fig. 2. (a, b) Turbidity and (c, d) DLS analysis results. (a) The δ_{700} and (c) $<R_h>_0$ after CO_2/N_2 purge, as a function of temperature in dark. (b) A change in the δ_{700} and (d) $<R_h>_0$ upon repeated 30 min of CO_2/N_2 purge, in dark or irradiating with an ultraviolet lamp.

[20–22], and ether oxygens as well [33], which could reduce hydrogen bonding of polymers with water and thus the hydrophilicity that lead to the drop of transmittance [34]. Since this subtle variation can also disrupt counterbalance of hydrophilic and hydrophobic forces in microgels, which is a key factor responsible for thermo-responsiveness [39,40], then, temperature-dependence on the δ_{700} was studied. Results indeed show an increased δ_{700} at elevated temperatures (Fig. 2a), representing a possible transition at *ca.* 54.6 °C upon N_2 purge (Fig. S10 in Supporting information); the transition temperature drops to *ca.* 47.5 °C, 43.3 °C and 41.8 °C, respectively, after a 30 s, 5 min and 30 min of CO_2 purge (Figs. S10 and S11 in Supporting information). Those results demonstrate that the microgels are CO_2-responsive. In further cyclic tests (Fig. 2b and Fig. S9), purge again with N_2 following the CO_2 purge, the δ_{700} cannot fully recover. The recovery ratio R_δ is *ca.* 5% at 20.0 °C, as estimated by $R_\delta = (\delta_{CO_2}\text{-}\delta_{N_2})/(\delta_{CO_2}\text{-}\delta_0)$, in which δ_0 is the initial δ_{700}, and δ_{CO_2} is the δ_{700} after a CO_2 purge and δ_{N_2} is that after one cycle of CO_2/N_2 purge. A larger R_δ appears at the higher temperature (Fig. 2b and Fig. S12 in Supporting information). However, unsatisfying recovery ratios were recorded over the range of temperatures for turbidity analysis (20–80 °C; *e.g.*, $R_\delta \approx 45\%$ at 80.0 °C), demonstrating a poor reversibility.

The reversibility of CO_2-responsiveness can be improved by irradiation to an ultraviolet lamp (offering 30.0 W/cm^2 area light of a wavelength 365 nm) (Fig. 2b; keeping the temperature at the set value while turning off gas purge and the lamp for rapid measurements, the same below). This seems to be realized by altering the variations on the δ_{700} under CO_2/N_2 purge. Compared with results measured in dark, when the light was applied, the rising extent of the δ_{700} upon purge with CO_2 became lower, whereas the reducing extent of the δ_{700} became more significant upon purge again with N_2. Taken together the two variation manners, light-mediated CO_2-responsiveness could be achieved and the R_δ approached 100% at 20.0 °C, indicating good reversibility under a mild condition. Similar results were obtained at other temperatures in the range of 20–80 °C (*e.g.*, at 80.0 °C, Fig. 2b and Fig. S12).

An examination on the observed δ_{700} change may raise a few questions. The first possible question associates with aggregation: may the recorded δ_{700} relate to aggregation of microgels? It has been reported that macromolecular clews in solutions below a critical concentration (*ca.* 0.1 wt%) can conserve individuality [41]. Given that the δ_{700} was recorded on dispersions of a much lower concentration (0.015 wt%), aggregation of microgels may be excluded. This hypothesis is supported by particle dynamics, through characterizing particle diffusion using an exponent P that is obtained by diffusing wave spectroscopy. If aggregation occurred, a change on particle dynamics can be reflected in a change from freely diffusive ($P \approx 1$) to subdiffusive motion ($P < 0.8$) [42]. Here, a constant P of *ca.* 1 is obtained in the temperature range of 20–80 °C (Fig. S13 in Supporting information), confirming that the microgels did not lose individuality. The δ_{700} change reflects transitions of individual microgels. To provide a direct evidence, dynamic light scattering (DLS) was used to monitor the average hydrodynamic radius $<R_h>_0$, which is "equivalent sphere radius" [43,44] that is obtained by angular extrapolation of apparent diffusion coefficient of microgels. As expected, the equilibrated $<R_h>_0$ decreased as CO_2 purge time increasing (Fig. 2c), rendering a large volumetric swelling ratio $SW(N_2/CO_2) = (<R_h>_0(\text{initial}, N_2)/<R_h>_0(\text{after a 30 min of } CO_2 \text{ purge}))$ [3] of 17.9 at 20.0 °C in dark, indicating a high CO_2-responsivity. For each case of the same CO_2 purge time, the microgels deswelled at elevated temperatures until a sharp but continuous change around the δ_{700} transition temperature (Fig. S14 in Supporting information), resulting in a smaller difference between $<R_h>_0$ under N_2/CO_2 purge at the higher temperature (*e.g.*, $SW(N_2/CO_2) = 3.5$ at 80.0 °C). When the light was applied, full reversible CO_2-responsiveness was also observed (Fig. 2d), indicating existence of light-mediated CO_2-responsiveness on individual microgels.

The second possible question relates to the observation of light-mediated CO_2-responsiveness of the microgels. The characteristics of the change in δ_{700} and $<R_h>_0$ upon CO_2/N_2 purge in light is highly reminiscent of consequences of photoexcitation [45–47], which has been reported previously on metallopolymers that the internal energy absorbed from an exciting radiation could be lost by nonradiative processes among others [23,35]. Internal conversion (driven by the kinetic coupling between electronic states; Fig. S15 in Supporting information) and the intersystem crossing (mediated by the spin–orbit coupling) are main intramolecular nonradiative processes [45–47]. Note that most organics following photoexcitation undergo rapid internal conversion to the lowest excited singlet state (S_1) [46,47], but the internal conversion from S_1 to the lowest singlet state S_0 is relatively slow, allowing time to promote intersystem crossing rapidly of S_1-state to the lowest triplet state T_1 of organometallics *via* heavy-atom effect without significantly perturbing the excited-state dynamics [48], which facilitates formation of T_1-state of metallapentalenes [24,49]. As singlet and triplet states are distinct in nature [45], particularly (anti)aromaticity [28–30,47], the above explanation should be generalized for light-mediated CO_2-responsiveness of the microgels. In a density functional theory (DFT) calculation, metallapentalene with osmium center and with a strong π-acceptor ligand (like CO; Scheme 1) was proposed to be aromatic in S_0-state, whereas antiaromatic in T_1-state [49]. (Anti)aromaticity refers to multidimensional manifestation in energetics, reactivity, electron delocalization and other properties, all of which in turn have been used to define numerous indices of (anti)aromaticity [24,28–30]. For instance, the gain of aromaticity in FLP groups for the activation of asmall molecule (*e.g.*, CO_2) may result in a gain of stability in both the corresponding transition state (leading to a lower barrier transformation), and in final adduct (making the process thermodynamically more favorable) [26,27]. Thereby, it appears that light-mediated CO_2-responsiveness is driven by the loss of aromaticity from initial photoexcitation and concurrent formation of a less reactive, antiaromatic excited state of relatively low CO_2 binding affinity, and by subsequent relief of antiaromaticity that can enhance CO_2 removal upon N_2 purge in light, that is, the origination of good reversibility. In comparison with results recorded at the same temperature in dark, the decrease in δ_{700} (Fig. 2b) and increase in $<R_h>_0$ (Fig. 2d) upon CO_2 purge in light should support

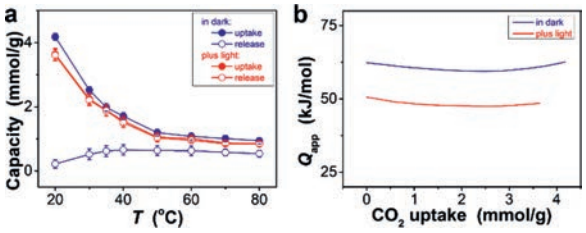

Fig. 3. (a) CO_2 uptake capacity of the microgels under 1 atm CO_2 pressure at different temperatures, and the corresponding CO_2 release capacity upon N_2 purge at the same temperature for the uptake. Spontaneous capture from the solution without microgels was subtracted. (b) The apparent isosteric heat of CO_2 uptake (Q_{app}) at 20.0 °C.

the suppression of light for CO_2 binding, thus, indirectly reflect the feasibility of the explanation.

Given that the difference in CO_2 binding affinity can lead to a change in CO_2 uptake/release capacity [13–17], single-gas uptake-release experiments were performed. Fig. 3a indicates a larger CO_2 uptake capacity of the microgels in dark than that acquired in light at the same temperature of 20.0 °C, in agreement with the variation in the δ_{700} and $<R_h>_0$ upon CO_2 purge between in dark and in light. Experiments at other temperatures in the range of 20–80 °C and over a pressure range from 0.1 atm to 1 atm indicated similar results (Fig. S16 in Supporting information). These results also demonstrate the dominate impact of the intersystem crossing, although the influence of the heat generated by internal conversion is ineluctable. Based on those isotherms (Fig. S17 in Supporting information), apparent isosteric heat of CO_2 uptake (Q_{app}) for the microgels was estimated (Fig. 3b) [50]. The reduction on the Q_{app} was apparent on light exposure (*e.g.*, $Q_{app} \approx 50.6$ kJ/mol at zero loading and at 20.0 °C), compared to that in dark ($Q_{app} \approx 62.4$ kJ/mol at zero loading at 20.0 °C). It is reasonable that light had acted as a mediator to tune CO_2 binding affinity [13–16]. This is further supported by CO_2 removal ability (Fig. 3a). Over 95% of the CO_2 captured in light was released by N_2 purge also in light at the same temperature, standing in contrast against barely or partial (< 54%) release in case of uptake/release in dark (Fig. S18 in Supporting information). The observation is consistent with turbidity and DLS results, well connecting light-mediated CO_2-responsiveness to CO_2 uptake/release capacity.

Further optimizing the experiments *via* a combination of CO_2 capture in dark and CO_2 removal in light, the former can enable a large CO_2 uptake capacity of *ca.* 4.2 mmol/g under 1 atm CO_2 pressure at 20.0 °C, and the latter allows partial release (by keeping CO_2 purge while exposing to light) or full release (by N_2 purge in light) of CO_2 under ambient pressure at 20.0 °C (Fig. 4a). This finding is curious, since both CO_2 capture of high capacity and CO_2 removal of good reversibility are realized under a mild condition, without large temperature swings (Fig. S19 in Supporting information) that is required for CO_2 uptake/release reported previously (Table S2 in Supporting information) [1–18]. It is the change in the heat of uptake that produces large differences in binding of CO_2 to polymers: CO_2 capture in dark favors the formation of strong interactions (the Q_{app} above 60 kJ/mol; *e.g.*, metal complexes), and light exposure facilitates weak interactions (the Q_{app} below 60 kJ/mol; *e.g.*, quadrupole-π) coming to dominate [20,51,52]. As strong interactions favor CO_2 capture from dilute sources, one may wonder how low a CO_2 level can induce an effective CO_2-responsiveness. To this end, the dispersion was bubbled with CO_2/N_2 mixed-gases (Fig. 4b). Distinctly, the microgels could respond to CO_2 at low CO_2 levels, as evidenced by attainment of a plateau of CO_2 uptake capacity ≥3.9 mmol/g even with CO_2 level lower down to 30 vol% in dark (Fig. 4c); correspondingly, the microgels deswelled, with $<R_h>_0 \leq 68.2$ nm (Fig. 4d) or SW(N_2/CO_2) ≥ 13.1 (Fig. S20 in Supporting information). If we defined the effective CO_2-responsiveness as a CO_2 level under which a 10% $<R_h>_0$ change was measured, the critical CO_2 level was *ca.* 1 vol% in dark, which increased to *ca.* 70 vol% in light. This also indicates that, for the mixed-gas containing 1–70 vol% CO_2, the microgels could effectively respond in dark, and nearly recover by simply exposing to light.

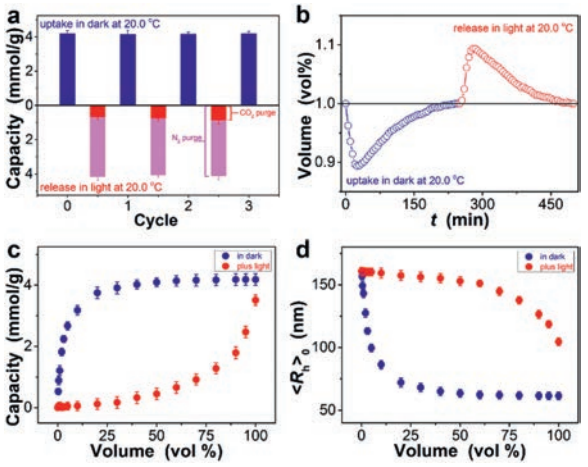

Fig. 4. (a) CO_2 capacity of uptake in dark upon CO_2 purge, and that release in light upon CO_2 purge or N_2 purge. (b) Time-domain volume of CO_2 in the gas flow, upon purge with 1 vol% CO_2 gas. (c) CO_2 uptake capacity in dark and in light, upon purge with CO_2/N_2 mixed-gases, and (d) changes in the $<R_h>_0$ after the corresponding treatments. Spontaneous uptake from the solution without any microgels was subtracted. All tests were under ambient pressure at 20.0 °C.

Light-mediated CO_2-responsiveness was also observed on spherical metallopolymer microgels (Fig. S21 in Supporting information). These spherical microgels could also exhibit both CO_2 capture of high capacity (*ca.* 3.9 mmol/g under 1 atm at 20.0 °C in dark) and CO_2 removal of good reversibility (by exposing to light) under a mild condition (Fig. S22 in Supporting information).

In summary, we demonstrate the concept of mediating CO_2-responsiveness through tuning CO_2 binding affinity by using side-chain type metallopolymers containing metalla-aromatics as CO_2-responsive moieties on microgels. Studies on the dilute aqueous dispersions of these microgels in dark indicate high CO_2-responsivity, but poor reversibility upon N_2 purge, which can be improved by applying light exposure. This light-mediated CO_2-responsiveness can be elucidated by the loss of aromaticity from initial photoexcitation and concurrent formation of a less reactive, antiaromatic excited state of relatively low CO_2 binding affinity, and by subsequent relief of antiaromaticity that can enhance CO_2 removal. Our results underscore the vast potential of bridging metalla-aromatic chemistry and polymer science to enable both CO_2 capture of high capacity and CO_2 removal of good reversibility under a mild condition, providing a novel strategy for the design of valuable materials that can effectively, reversibly respond to dilute CO_2.

Declaration of competing interest

The authors declare that they have no known competing financial interests or personal relationships that could have appeared to influence the work reported in this paper.

Acknowledgments

This work is supported by National Natural Science Foundation of China (Nos. 21774105, 21805164, 20923004), Chuying Plan Youth

Top-notch Talents of Fujian Province, and National Fund for Fostering Talents of Basic Science (No. J1310024).

References

[1] Q. Yan, R. Zhou, C.K. Fu, et al., Angew. Chem. Int. Ed. 50 (2011) 4923–4927.
[2] D.H. Han, X. Tong, O. Boissière, Y. Zhao, ACS Macro Lett. 1 (2012) 57–61.
[3] H. Yu, K. Imamura, M. Yue, G. Inoue, Y.Y. Miura, J. Am. Chem. Soc. 134 (2012) 18177–18180.
[4] K.C. Jie, Y. Yao, X.D. Chi, F.H. Huang, Chem. Commun. 50 (2014) 5503–5505.
[5] K.C. Jie, Y.J. Zhou, Y. Yao, B.B. Shi, F.H. Huang, J. Am. Chem. Soc. 137 (2015) 10472–10475.
[6] K. Jie, Y. Zhou, Y. Yao, B. Shi, F. Huang, J. Am. Chem. Soc. 137 (2015) 10472–10475.
[7] A. Darabi, P.G. Jessop, M.F. Cunningham, Chem. Soc. Rev. 45 (2016) 4391–4436.
[8] Q. Zhang, L. Lei, S.P. Zhu, ACS Macro Lett. 6 (2017) 515–522.
[9] H.B. Liu, S.J. Lin, Y.J. Feng, P. Theato, Polym. Chem. 8 (2017) 12–23.
[10] B.X. Jiang, Y.C. Zhang, X.D. Huang, et al., Ind. Eng. Chem. Res. 58 (2019) 15088–15108.
[11] M.F. Cunningham, P.G. Jessop, Macromolecules 52 (2019) 6801–6816.
[12] S.Y. Wang, Q.H. Liu, L. Li, M.W. Urban, Macromol. Rapid Commun. (2021) 2100054.
[13] B.S. Zheng, J.F. Bai, J.G. Duan, L. Wojtas, M.J. Zaworotkoet, J. Am. Chem. Soc. 133 (2011) 748–751.
[14] F. Ding, X. He, X.Y. Luo, et al., Chem. Commun. 50 (2014) 15041–15044.
[15] X.Y. Luo, X.Y. Chen, R.X. Qiu, et al., Dalton Trans. 48 (2019) 2300–2307.
[16] P. Das, S.K. Mandal, Chem. Mater. 31 (2019) 1584–1596.
[17] L. Chen, R.J. Liu, Q. Yan, Angew. Chem. Int. Ed. 57 (2018) 9336–9340.
[18] L. Chen, R.J. Liu, X. Hao, Q. Yan, Angew. Chem. Int. Ed. 58 (2019) 264–268.
[19] D.W. Stephan, G. Erker, Angew. Chem. Int. Ed. 54 (2015) 6400–6441.
[20] M. Aresta, A. Angelini. The carbon dioxide molecule and the effects of its interaction with electrophiles and nucleophiles, in: X.B. Lu (Ed.), Carbon Dioxide and Organometallics, Vol. 53, Springer Nature Switzerland AG, 2016, pp. 1-38.
[21] Y.L. Wang, D. Astruc, A.S. Abd-El-Aziz, Chem. Soc. Rev. 48 (2019) 558–636.
[22] E.J. Kim, R.L. Siegelman, H.Z. Jiang, A.C. Forse, J.R. Long, Science 369 (2020) 392–396.
[23] C.Q. Zhu, S.H. Li, M. Luo, et al., Nat. Chem. 5 (2013) 698–703.
[24] D.F. Chen, Y.H. Hua, H.P. Xia, Chem. Rev. 120 (2020) 12994–13086.
[25] I. Fernández, F.M. Bickelhaupt, Chem. Soc. Rev. 43 (2014) 4953–4967.
[26] J.J. Cabrera-Trujillo, I. Fernández, Chem. Commun. 55 (2019) 675–678.
[27] D.L. Zhuang, A.M. Rouf, Y.Y. Li, C. Dai, J. Zhu, Chem. Asian J. 15 (2020) 266–272.
[28] M. Rosenberg, C. Dahlstrand, K. Kilså, H. Ottosson, Chem. Rev. 114 (2014) 5379–5425.
[29] Y.M. Sung, M.C. Yoon, J.M. Lim, et al., Nat. Chem. 7 (2015) 418–422.
[30] B. Oruganti, P.P. Kalapos, V. Bhargav, G. London, D. Bo, J. Am. Chem. Soc. 142 (2020) 13941–13953.
[31] M.C. Yue, Y. Hoshino, Y. Miura, Chem. Sci. 6 (2015) 6112–6123.
[32] P.D.L. Werz, J. Kainz, B. Rieger, Macromolecules 48 (2015) 6433–6439.
[33] X.F. Wang, H.J. Qiu, Q.S. Wu, et al., ACS Macro Lett. 9 (2020) 1611–1616.
[34] F. Lu, X.Z. Lin, Q.S. Wu, et al., ACS Macro Lett. 9 (2020) 266–271.
[35] Z.Y. Lu, J.X. Chen, H.P. Xia, Chin. J. Org. Chem. 37 (2017) 1181–1188.
[36] M. Yan, Y. Kawamata, P.S. Baran, Chem. Rev. 117 (2017) 13230–13319.
[37] S.T. Farrell, C.B. Breslin, Electrochim. Acta 49 (2004) 4497–4503.
[38] Q.J. Chen, R. Ranaweera, L. Luo, J. Phys. Chem. C 122 (2018) 15421–15426.
[39] C.D. Jones, L.A. Lyon, Langmuir 19 (2003) 4544–4547.
[40] R. Pelton, Adv. Colloid Interface Sci. 85 (2000) 1–33.
[41] C. Wu, J. Polym. Sci. Part B: Polym. Phys. 32 (1994) 1503–1509.
[42] S. Romer, F. Scheffold, P. Schurtenberger, Phys. Rev. Lett. 85 (2000) 4980–4983.
[43] B. Chu, Laser Light Scattering, 2nd ed., Academic Press, New York, 1991.
[44] Q.J. Chen, H. Zhao, T. Ming, J.F. Wang, C. Wu, J. Am. Chem. Soc. 131 (2009) 16650–16651.
[45] H. Lischka, D. Nachtigallová, A.J.A. Aquino, et al., Chem. Rev. 118 (2018) 7293–7361.
[46] H.S. Jung, P. Verwilst, A. Sharma, et al., Chem. Soc. Rev. 47 (2018) 2280–2297.
[47] G. McKay, Processes Impacts 22 (2020) 1139–1165.
[48] K.N. Solovyov, E.A. Borisevich, Phys. Usp. 48 (2005) 231–253.
[49] D.D. Chen, D.W. Szczepanik, J. Zhu, M. Solà, Chem. Eur. J. 26 (2020) 12964–12971.
[50] O.L.I. Brown, J. Chem. Educ. 28 (1951) 428.
[51] C.A. Trickett, A. Helal, B.A. Al–Maythalony, et al., Nat. Rev. Mater. 2 (2017) 1–16.
[52] P.M. Bhatt, Y. Belmabkhout, A. Cadiau, et al., J. Am. Chem. Soc. 138 (2016) 9301–9307.